

Chapter 1

Single-Electron Tunneling and the Fluctuation Theorem

Y. Utsumi¹, D. S. Golubev², M. Marthaler³, T. Fujisawa^{4,5}, and
Gerd Schön^{2,3}

¹*Institute for Solid State Physics, University of Tokyo, Kashiwa, Chiba
277-8581, Japan*

²*Institut für Nanotechnologie, Karlsruhe Institute of Technology, 76021
Karlsruhe, Germany*

³*Institut für Theoretische Festkörperphysik and DFG Center for
Functional Nanostructures (CFN), Karlsruhe Institute of Technology,
76128 Karlsruhe, Germany*

⁴*NTT Basic Research Laboratories, NTT Corporation,
Morinosato-Wakamiya, Atsugi 243-0198, Japan*

⁵*Research Center for Low Temperature Physics, Tokyo Institute of
Technology, Ookayama, Meguro, Tokyo 152-8551, Japan*

Experiments on the direction-resolved full-counting statistics of single-electron tunneling allow testing the fundamentally important Fluctuation Theorem (FT). At the same time, the FT provides a frame for analyzing such data. Here we consider tunneling through a double quantum dot system which is coupled capacitively to a quantum point contact (QPC) detector. Fluctuations of the environment, including the shot noise of the QPC, lead to an enhancement of the effective temperature in the FT. We provide a quantitative explanation of this effect; in addition we discuss the influence of the finite detector bandwidth on the measurements.

1.1. Introduction

The second law of thermodynamics states that the entropy of a macroscopic system driven out of equilibrium grows with time, and the dynamics of such a system is irreversible. The entropy of a mesoscopic system also grows in the long-time limit, but it may decrease over sufficiently short periods of time. Hence, the entropy production ΔS during a time interval τ

2 *Y. Utsumi*¹, *D. S. Golubev*², *M. Marthaler*³, *T. Fujisawa*^{4,5}, and *Gerd Schön*^{2,3}

is a random variable, characterized by a distribution $P_\tau(\Delta S)$. The ‘Fluctuation Theorem’ (FT)¹ states that the probabilities of positive and negative entropy changes at sufficiently long τ are related by

$$\frac{P_\tau(\Delta S)}{P_\tau(-\Delta S)} = \exp(\Delta S). \quad (1.1)$$

Remarkably, this simple and universal relation remains valid even far from equilibrium. It has been proven for thermostated Hamiltonian systems,¹ Markovian stochastic processes,^{2–4} quantum systems,⁵ and mesoscopic conductors.^{6–11} The FT is fundamentally important for transport theory. One of its consequences is the Jarzynski equality,^{12,13} which in turn leads to the 2nd law of thermodynamics. It also leads to the fluctuation-dissipation theorem and Onsager symmetry relations,¹⁴ as well as to their extensions to nonlinear transport.^{6–11}

The FT was first verified in an experiment measuring the distribution of the work done on a colloidal particle placed in a water flow and trapped by an optical tweezer.¹⁵ By monitoring the position fluctuations it is possible to estimate the work done on the particle. For this classical experiment, as well as for other related ones performed at room temperature,¹⁶ the thermal fluctuations are quite large and the FT has been confirmed. In contrast, experiments for mesoscopic quantum systems¹⁷ were lacking until very recently.^{18,19}

Let us now discuss the implications of FT for mesoscopic systems. The first experimental test of the FT applied to single-electron transport has been performed recently in Ref.^{18,20} A system of two coupled quantum dots in a 2DEG at the GaAs/AlGaAs interface was operated in the Coulomb blockade regime. (The single-electron charging energy of a single dot was of the order of 100 μeV , and the sample was cooled to 100 milli-Kelvin.) The single-electron tunneling through the double dot system was detected via the current through a nearby quantum point contact (QPC). The time resolution of the readout was better than 0.1 ms. By using an asymmetric setup the direction of tunneling could be resolved, and the probability distribution of forward and backward tunneling processes could be determined.

The entropy production in this experiment is related to Joule heating and reads $\Delta S = qeV_S/k_B T$, where q is the number of electrons (with charge e) transferred through the conductor during time τ and V_S is the bias voltage. Hence the FT can be formulated in terms of the distribution of transferred charge $P_\tau(q)$ at sufficiently long times, $\tau \gtrsim e/I$, where I is

the current, as follows

$$\frac{P_{\tau}(q)}{P_{\tau}(-q)} = \exp\left(\frac{qeV_S}{k_B T}\right). \quad (1.2)$$

Unlike in classical systems, the fluctuations of the charge transferred through the quantum dots are strongly affected by the environment (phonons and electromagnetic environment) and by the measurement back-action. In what follows we discuss various environmental effects and demonstrate their importance for the interpretation of the experiment. We show that the non-equilibrium electromagnetic fluctuations caused by the non-equilibrium shot noise of the QPC detector lead to an apparent violation of the FT. However, we find the FT to be satisfied if we replace the temperature T in Eq. (1.2) by an enhanced effective temperature T^* , which we relate to the tunneling rates for the various relevant processes. We also study the effect of finite bandwidth of the detector^{21–23} and show that in the parameter regime of our experiment, this effect may also be accounted for by an effective temperature.

The paper is organized as follows. In Sec. 1.2, we briefly discuss the experimental results. In Sec. 1.3, we discuss the theory relevant for our experiment assuming a perfect detector. In Sec. 1.4, we discuss the effect of the environment. The realistic case, where the time resolution of the detector is limited by its bandwidth, will be discussed in Sec. 1.5. There we will show that it is still possible to recover the FT with properly corrected tunneling rates. In Sec. 1.6, we show how the tunneling rates are determined experimentally and how the finite bandwidth of the detector affects the experimentally obtained value. Section 1.7 summarizes our discussion.

1.2. Experimental test of the FT in single-electron counting

Most of the experiments on single-electron counting are performed with a single quantum dot capacitively coupled to a QPC detector.²⁴ In this case the QPC current switches between the two values corresponding to an occupied and an empty quantum dot. Such a detector cannot resolve the direction of the electron tunneling and, therefore, is not suitable for testing the FT. The simplest system which does resolve the direction of the tunneling consists of two serially coupled quantum dots which are asymmetrically coupled to a QPC detector²⁰ (Fig. 1.1 a). The left and right gate voltages, V_{GL} and V_{GR} , applied to the quantum dots are tuned in such a way that only three charge states of the DQD need to be considered. In

4 Y. Utsumi¹, D. S. Golubev², M. Marthaler³, T. Fujisawa^{4,5}, and Gerd Schön^{2,3}

the experiment²⁰ those states are $|D\rangle$ (both dots are occupied), $|L\rangle$ (left dot is occupied by one electron) and $|R\rangle$ (right dot is occupied). Accordingly, the current through the QPC, which is coupled asymmetrically to the DQD, switches between three different values (Fig. 1.1 b). This setup allows distinguishing electron tunneling in different directions and between the dots and leads.

From the time trace of the current taken during time τ one obtains the distribution of transferred charges between the two dots, $P_\tau(q)$, an example of which is shown in the inset of Fig. 1.2. In Fig. 1.2 we perform a test of the FT (1.2). The combination $\ln[P_\tau(q)/P_\tau(-q)]$ depends indeed linearly on the transferred charge q with a slope $eV_S/k_B T^*$. Here $V_S = 300 \mu\text{V}$ is the applied DQD bias voltage, but the effective temperature $T^* = 1.37 \text{ K}$ fitting the data (dashed line) strongly exceeds the bath temperature of the leads of $T = 130 \text{ mK}$ (dot-dashed line).

In order to understand this apparent violation, we have to consider the total system. The FT for the system composed of the DQD and QPC should be formulated in terms of the joint probability distribution $P_\tau(q, q')$, where q and q' charges are transmitted through the DQD and the QPC,

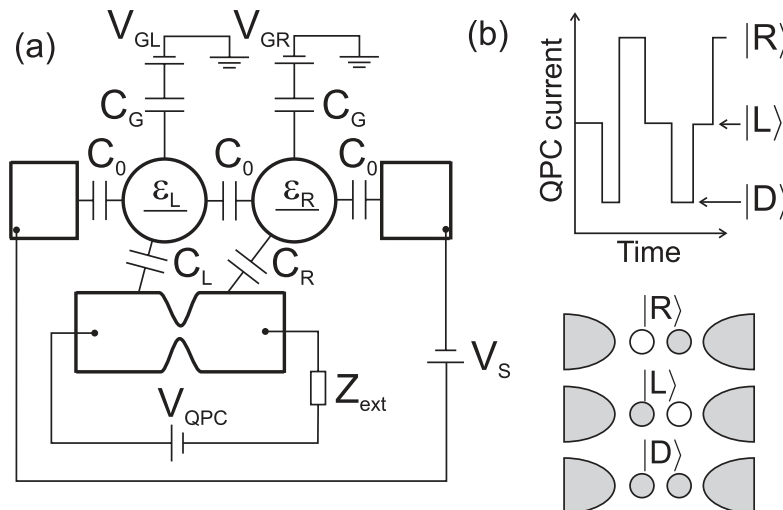


Fig. 1.1. (a) Setup of the system with two quantum dots (DQD) with single-level energies ϵ_L and ϵ_R coupled to a quantum point contact (QPC). (b) The QPC current switches between three values corresponding to the three charge states of the DQD.

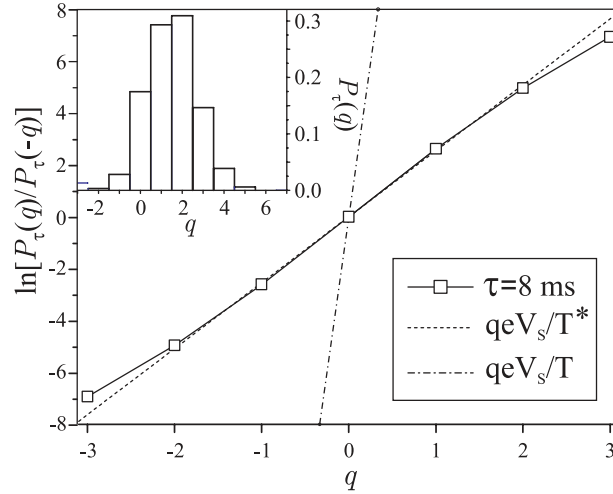


Fig. 1.2. Test of FT (1.2) with the measurement time $\tau = 8$ ms. Lines with squares: logarithm of lhs of Eq. (1.2); dashed line: $qeV_S/k_B T^*$ with $T^* = 1.37$ K; dot-dashed line: $qeV_S/k_B T$. Inset: the distribution $P_\tau(q)$ at $\tau = 4$ ms.

respectively (Fig. 1.3).⁹ It satisfies

$$P_\tau(q, q') = \exp\left(\frac{qeV_S + q'eV_{QPC}}{k_B T}\right) P_\tau(-q, -q'). \quad (1.3)$$

Since only the number of charges q is measured, Eq. (1.3) should be summed over q' . As a result, the right hand side deviates from $\exp[eV_S/k_B T] P_\tau(-q)$ (except for $V_{QPC} = 0$), which appears to violate the FT. In the following section we will provide a more detailed discussion and further the reasoning why the FT is recovered when we introduce the effective temperature.

1.3. FT in the single-electron transport

In the experiment, electrons tunnel through the dots sequentially. The system is then fully characterized by the vector of the occupation probabilities of the DQD charge states, $\mathbf{p}^T = (p_L, p_R, p_D)$, which satisfies the following master equation

$$\partial_t \mathbf{p} = \Gamma(\lambda) \mathbf{p}. \quad (1.4)$$

6 *Y. Utsumi*¹, *D. S. Golubev*², *M. Marthaler*³, *T. Fujisawa*^{4,5}, and *Gerd Schön*^{2,3}

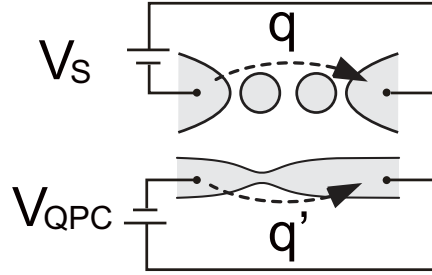


Fig. 1.3. Schematic picture of the DQD capacitively coupled to the QPC illustrating the apparent violation of the FT. In addition to the source-drain bias V_S applied to the QDQ the voltage V_{QPC} is applied to the QPC. Thus, the total system is a 4-terminal setup, and the FT should be formulated for the joint probability distribution of transmitted charges through the QPC and DQD, $P(q, q')$. The FT for $P(q)$ is valid only for $V_{QPC} = 0$.

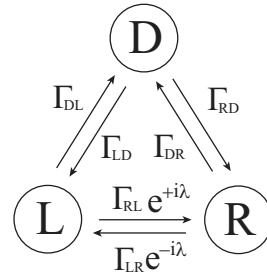


Fig. 1.4. The relevant transition processes. Circles represent the double-dot states and arrows the directions of the transitions. The factor $e^{\pm i\lambda}$, needed for the Full Counting Statistics, indicates that the electron number is ‘counted’ at the center barrier.

Here the transition matrix is given by,

$$\mathbf{\Gamma}(\lambda) = \begin{pmatrix} -\Gamma_{RL} - \Gamma_{DL} & \Gamma_{LR}e^{-i\lambda} & \Gamma_{LD} \\ \Gamma_{RL}e^{i\lambda} & -\Gamma_{LR} - \Gamma_{DR} & \Gamma_{RD} \\ \Gamma_{DL} & \Gamma_{DR} & -\Gamma_{LD} - \Gamma_{RD} \end{pmatrix}. \quad (1.5)$$

Figure 1.4 indicates six transitions with Γ_{ij} between three charge states. Following the recipe of the full-counting statistics (FCS) of Bagrets and Nazarov,²⁵ we introduced the counting field λ , which keeps track of the electrons transferred through the tunnel barrier between the two quantum dots (Fig. 1.4). Then the probability distribution of the charge transferred

through this barrier during the time τ is given by the Fourier transform

$$P_\tau(q) = \int_{-\pi}^{\pi} \frac{d\lambda}{2\pi} e^{-i\lambda q} \mathcal{Z}_\tau(\lambda), \quad (1.6)$$

where

$$\mathcal{Z}_\tau(\lambda) = p_L(\tau) + p_R(\tau) + p_D(\tau), \quad (1.7)$$

is the characteristic function. In the long time limit $\tau \gg I/e$, the characteristic function takes the form $\mathcal{Z}(\lambda) \sim e^{\tau \mathcal{F}(\lambda)}$, where $\mathcal{F}(\lambda)$ is the eigenvalue of the matrix $\mathbf{\Gamma}(\lambda)$ with the largest real part. The function $\mathcal{F}(\lambda)$ has to be found from the characteristic equation

$$0 = \det[\mathbf{\Gamma}(\lambda) - \mathcal{F} \mathbf{I}] = \mathcal{F}^3 + K\mathcal{F}^2 + K'\mathcal{F} + \Gamma_{DR}\Gamma_{RL}\Gamma_{LD}(e^{i\lambda} - 1) + \Gamma_{DL}\Gamma_{LR}\Gamma_{RD}(e^{-i\lambda} - 1), \quad (1.8)$$

where K and K' are parameters independent of the counting field,

$$K = \sum_{i \neq j} \Gamma_{ij}, \quad K' = \sum_{i \neq j} \sum_k \Gamma_{ik}\Gamma_{kj} + \sum_{i \neq j} \sum_k \Gamma_{ki}\Gamma_{kj}/2. \quad (1.9)$$

Without solving this equation we observe that $\mathcal{F}(\lambda)$ and hence $\mathcal{Z}(\lambda)$ in the long time limit satisfy the identity

$$\mathcal{Z}(\lambda) = \mathcal{Z} \left(-\lambda + i \frac{eV_S}{k_B T^*} \right), \quad (1.10)$$

where the effective temperature T^* is

$$T^* = \frac{eV_S}{k_B \ln w}, \quad (1.11)$$

$$w = \frac{\Gamma_{DR}\Gamma_{RL}\Gamma_{LD}}{\Gamma_{DL}\Gamma_{LR}\Gamma_{RD}}. \quad (1.12)$$

Performing the inverse Fourier transformation of Eq. (1.10), we arrive at the relation (1.2) for the distribution $P_\tau(q)$ with T being replaced by T^* .

One can demonstrate¹⁸ that the effective temperature (1.11) is equal to the base temperature, $T^* = T$, when the tunneling rates Γ_{ij} satisfy the detailed balance relation

$$\frac{\Gamma_{ij}}{\Gamma_{ji}} = \exp \left(\frac{\Delta_j - \Delta_i}{k_B T} \right), \quad (1.13)$$

where Δ_j are the electrochemical potentials of the charge states of the DQD. In real experiments the QPC is biased and generates a non-equilibrium shot noise. Under these conditions the detailed balance is violated and, as we

8 *Y. Utsumi*¹, *D. S. Golubev*², *M. Marthaler*³, *T. Fujisawa*^{4,5}, and *Gerd Schön*^{2,3}

will show later in Sec. 1.4, we have $T^* > T$. Although the canonical form of the FT (1.2) is violated in this case, the more general form (1.1) still holds. The reason is the underlying simplicity of the considered system, in which a forward transfer of a single electron occurs only through the following cycle of transitions $|D\rangle \rightarrow |L\rangle \rightarrow |R\rangle \rightarrow |D\rangle$ (see Fig. 1.4). It enables us to introduce the macroscopic affinity $\ln w$ uniquely.^{2-4,26} For a general system with more cycles in its state transition diagram, the FT holds only when the affinities for all cycles associated with current flow into/out of a particular lead coincide.^{4,26} Later in Sec. 1.5, we will show that a detector with finite bandwidth leads to a violation of this condition.

1.4. Effects of backaction and environments

Mesoscopic electron transport suffers from environmental effects. In GaAs nanostructures, acoustic phonons strongly couple to electrons via the deformation potential and the piezoelectric coupling.²⁷ For a QPC measurement, one cannot avoid the Coulomb interaction between the dots and QPC leads, which is marked by C_L and C_R in Fig. 1.1 a.^{22,28,29} This interaction is unwanted and causes a measurement backaction, since the nonequilibrium QPC shot noise leads to QD level fluctuations. In addition, the external circuit acts as the electromagnetic environment, which further affects both of the DQD and QPC.

Such environmental effects can be accounted for by the so-called $P(E)$ -theory³⁰ and more systematically by using the real-time diagrammatic technique.³¹ The phonon and electromagnetic environments, as well as the nonequilibrium QPC current noise generate QD level fluctuations, δV_L and δV_R . Then the tunnel rates connecting the three charge states are modified as,

$$\Gamma_{LR} = \pi |T_C|^2 P_C(E_L - E_R), \quad (1.14)$$

$$\Gamma_{DL} = \Gamma_R \int d\omega f(E_D - E_L - V_S/2 - \omega) P_R(\omega), \quad (1.15)$$

$$\Gamma_{RD} = \Gamma_L \int d\omega f(\omega - E_R + V_S/2 + E_D) P_L(\omega). \quad (1.16)$$

(Γ_{RL} , Γ_{LD} and Γ_{RD} are given in a similar manner). Here T_C is a tunnel matrix element describing the central barrier. The total energies of the charge states E_j include the electrostatic energy. The tunnel rates Γ_{DL} and Γ_{RD} are also affected by the thermal broadening of the reservoir levels through the Fermi distribution, $f(\omega) = 1/(1 + e^{\omega/k_B T})$.

The Fourier transform of the correlation function, $P_j(\omega) = \int dt e^{i\omega t} P_j(t)/(2\pi)$ induces additional broadening. It is determined by the fluctuating dot potentials, $\varphi_{L/R}(t) = \int^t dt' \delta V_{L/R}(t')$ and $\varphi_C = \varphi_R - \varphi_L$, as

$$P_j = \left\langle e^{i\hat{\varphi}_j(t)} e^{-i\hat{\varphi}_j(0)} \right\rangle = \exp \left[\int d\omega \frac{S_{\delta V_j}(\omega)(e^{-i\omega t} - 1)}{\omega^2} \right], \quad (1.17)$$

where the correlation function for the level fluctuations is determined by the properties of the environment.

For acoustic phonons the correlation function takes the following form

$$S_{\delta V_j}^{\text{ph}}(\omega) = \frac{A_j^{\text{ph}}(\omega)}{1 - e^{-\omega/k_B T}} \quad (1.18)$$

with super-ohmic, $A_C^{\text{ph}} \propto \omega^3$, or ohmic, $A_{L/R}^{\text{ph}} \propto \omega$, phonon spectral functions. Though phonons cause some additional broadening, for the experiment considered with low measurement current, $\langle I_{\text{QPC}} \rangle \approx 12 \text{ nA}$, the heating effect is negligible.²⁷ As long as the lattice and electronic systems are isothermal the detailed balance holds, and as a consequence the FT, Eq. (1.2), is satisfied.

The situation changes when the environment itself is out of equilibrium. Such an environment is generated by the QPC current fluctuations S_I^{QPC} , which give rise to the voltage fluctuation spectrum

$$S_{\delta V_j}^{\text{QPC}}(\omega) = \kappa_j |Z_t(\omega)|^2 S_I^{\text{QPC}}(\omega). \quad (1.19)$$

($\kappa_{L/R} = 1$, $\kappa_C = 4$). The non-symmetrized current noise of the QPC is given by

$$S_I^{\text{QPC}} = \frac{2}{R_K} \left[\sum_{\pm} \frac{\mathcal{T}_{\text{QPC}}(1 - \mathcal{T}_{\text{QPC}})(\omega \pm V_{\text{QPC}})}{1 - e^{-(\omega \pm V_{\text{QPC}})/k_B T}} + \frac{2 \mathcal{T}_{\text{QPC}}^2 \omega}{1 - e^{-\omega/k_B T}} \right]. \quad (1.20)$$

The impedance $Z_t(\omega) = 1/(i\omega \bar{C} + 1/\bar{R})$ characterizes the capacitive coupling between the QPC and the dot-level fluctuations δV_r . Here \bar{R} is written with the QPC resistance R_{QPC} as $\bar{R} = R_{\text{QPC}}/[1 + \bar{C}(C_L^{-1} + C_R^{-1})]$. The capacitance is $\bar{C} = (3C_0 + C_G)/2$, where the capacitances C_0 and C_G characterizes the coupling between dots, leads and gate electrodes (Fig. 1.1 a). For the experiment,²⁰ the QPC transparency for each spin is estimated as $\mathcal{T}_{\text{QPC}} = R_K/(2R_{\text{QPC}}) \approx 0.19$ and $V_{\text{QPC}} = 0.8 \text{ mV}$. Equation (1.19) is reduced to the equilibrium form Eq. (1.18), when $V_{\text{QPC}} = 0$ and the detailed balance is satisfied. However, for $V_{\text{QPC}} \neq 0$, the detailed balance and thus the FT, Eq. (1.2), are violated. Note that the violation is not contradict to the FT for the total DQD and QPC system, Eq. (1.3).

10 *Y. Utsumi*¹, *D. S. Golubev*², *M. Marthaler*³, *T. Fujisawa*^{4,5}, and *Gerd Schön*^{2,3}

Generally the electromagnetic environment suppresses the phase correlations. In the long-time limit, it decays exponentially $P_j(t) \approx \exp(-\Gamma_j^{\text{QPC}} t/2)$. For realistic parameters, $\bar{C} = 5\text{fF}$ and $\bar{C}(C_L^{-1} + C_R^{-1}) = 0.02$, the decay rate is rather big, $\Gamma_C^{\text{QPC}}/2 = \pi |Z_t(0)|^2 S_I(0) \approx 50\mu\text{eV}$. Even for the ideal case, i.e. there is no capacitive coupling between the QPC and the DQD, $C_{L/R} = 0$, the correlation function P_j decays exponentially. It is because of an *intrinsic* backaction often discussed in the context of the weak measurement.³² For the ideal case, the decay rate is,

$$\frac{\Gamma_C^{\text{QPC}}}{2} \approx -\frac{V_{\text{PC}} t}{\pi} \ln\left(\sqrt{\mathcal{T}_{|L\rangle}}\sqrt{\mathcal{T}_{|R\rangle}} + \sqrt{1-\mathcal{T}_{|L\rangle}}\sqrt{1-\mathcal{T}_{|R\rangle}}\right), \quad (1.21)$$

in the limit of $t \rightarrow \infty$ for $T \ll V_{\text{QPC}}$. Here $\mathcal{T}_{|s\rangle}$ means the transmission probability through the QPC when the DQD is in the state $|s\rangle$. However, for the experiment,²⁰ $I_{|L/R\rangle} \sim 12 \pm 0.1\text{nA}$, and thus we estimate $\Gamma_C^{\text{QPC}}/2 \sim 2.1\text{nV}$, which is negligible.

1.5. Effect of finite detector bandwidth

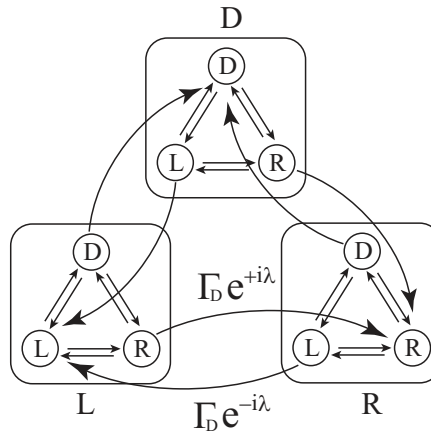


Fig. 1.5. State transition diagram for the double dot and the QPC detector with finite bandwidth. Circles represent the double-dot states and arrows show the directions of the transitions. The additional states representing the detector states (squares) are introduced. Within each square, transitions between all the dot states are possible. Between the 3 detector states, one-way transition, the relaxation from the ‘false’ detector state to the ‘true’ detector state, occurs.

In this section we discuss the effect of the finite bandwidth of the mea-

surement device on the FT. If the detector bandwidth is finite, the QPC current does not follow the switching between the DQD charge states immediately. Naaman and Aumentado²¹ proposed to describe such a system by doubling the number of states. In our system the DQD switches between three states $|D\rangle$, $|L\rangle$, $|R\rangle$, and the QPC current takes three values corresponding to those states $|D\rangle_{\text{QPC}}$, $|L\rangle_{\text{QPC}}$, $|R\rangle_{\text{QPC}}$. Then, we should describe the system by 9 states $|r\rangle|r'\rangle_{\text{QPC}}$ ($r, r' = L, R, D$), and we have to consider a vector of 9 occupation probabilities

$$\mathbf{p}^T = (p_{LL}, p_{RL}, p_{DL}, p_{LR}, p_{RR}, p_{DR}, p_{LD}, p_{RD}, p_{DD}), \quad (1.22)$$

where the first index refers to the state of the DQD and the second one to the value of the QPC current. As shown in Fig. 1.5, the detector will always change to the state corresponding to the dot-state. We model the fact that the detector needs a finite time for this switching, by introducing the detector rate Γ_D . For an ideal detector, $\Gamma_D \rightarrow \infty$, only the states are p_{LL} , p_{RR} and p_{DD} occur.

Because of the one-way transitions between detector states the considered system is outside the class discussed in Ref.⁴ In order to describe the experiment and the consequences for the FT we calculate the cumulant generating function. We introduce the master equation of the total system,

$$\partial_t \mathbf{p} = \mathbf{M}(\lambda) \mathbf{p}, \quad (1.23)$$

where the transition matrix is a 9×9 matrix,

$$\mathbf{M}(\lambda) = \begin{pmatrix} \Gamma(0) - \Gamma_{D2} - \Gamma_{D3} & \Gamma_{D1} e^{-i\lambda} & \Gamma_{D1} \\ \Gamma_{D2} e^{i\lambda} & \Gamma(0) - \Gamma_{D1} - \Gamma_{D3} & \Gamma_{D2} \\ \Gamma_{D3} & \Gamma_{D3} & \Gamma(0) - \Gamma_{D1} - \Gamma_{D2} \end{pmatrix}, \quad (1.24)$$

with sub-matrices given by

$$\mathbf{\Gamma}_{Di} = \Gamma_D \begin{pmatrix} \delta_{i1} & 0 & 0 \\ 0 & \delta_{i2} & 0 \\ 0 & 0 & \delta_{i3} \end{pmatrix}. \quad (1.25)$$

Note that the counting field is associated with the rate Γ_D . I.e., in the present model the switching of the QPC current are counted and not the transitions in the DQD system. Thus the model provides information about the experimentally accessible statistics of the detector rather than that of the DQD, which is not directly measurable. The model outlined above fits the measured higher cumulants for the single-dot case quite accurately.^{22,23}

12 *Y. Utsumi*¹, *D. S. Golubev*², *M. Marthaler*³, *T. Fujisawa*^{4,5}, and *Gerd Schön*^{2,3}

The FCS cumulant generating function \mathcal{F} is obtained by solving the the characteristic equation for the eigenvalue

$$\begin{aligned} 0 &= \det |\mathbf{M}(\lambda) - \mathcal{F} \mathbf{I}| \\ &= \det |\mathbf{M}(0) - \mathcal{F} \mathbf{I}| + \Gamma_+(\mathcal{F}) (e^{i\lambda} - 1) + \Gamma_-(\mathcal{F}) (e^{-i\lambda} - 1), \end{aligned} \quad (1.26)$$

where Γ_{\pm} are factorized as,

$$\Gamma_+(\mathcal{F}) = \Gamma_D^6 (x \Gamma_{DL} + \Gamma_{DL}^*) (x \Gamma_{LR} + \Gamma_{LR}^*) (x \Gamma_{RD} + \Gamma_{RD}^*), \quad (1.27)$$

$$\Gamma_-(\mathcal{F}) = \Gamma_D^6 (x \Gamma_{LD} + \Gamma_{LD}^*) (x \Gamma_{RL} + \Gamma_{RL}^*) (x \Gamma_{DR} + \Gamma_{DR}^*). \quad (1.28)$$

We introduced $x = \mathcal{F}/\Gamma_D$ and the corrected tunnel rates

$$\Gamma_{ij}^* = \Gamma_{ij} \left(1 + \frac{\Gamma_{ik} + \Gamma_{jk}}{\Gamma_D} \right) + \frac{\Gamma_{ik} \Gamma_{kj}}{\Gamma_D}, \quad (k \neq i, j). \quad (1.29)$$

In order to check whether the FT is satisfied, we consider the following ratio, generalizing w of the ideal case Eq. (1.12),

$$w^* = \frac{\Gamma_+(\mathcal{F})}{\Gamma_-(\mathcal{F})}. \quad (1.30)$$

The FT has to be exact if this ratio does not depend on \mathcal{F} . It is obvious that generally this is not the case and therefore the FT is violated. However, in two limits, for a fast detector $\Gamma_D \gg \Gamma_{ij}$ and for a slow detector $\Gamma_D \ll \Gamma_{ij}$, we are able to show analytically that the FT holds. In the former case, $\Gamma_D \gg \Gamma_{ij}$, we expand w^* in powers of $1/\Gamma_D$. Since $\mathcal{F}_D \sim \Gamma_{ij}$, we arrive at the following result

$$w^* = w + \frac{1-w}{\Gamma_D} \left(\frac{\Gamma_{LD} \Gamma_{DR}}{\Gamma_{LR}} + \frac{\Gamma_{RL} \Gamma_{LD}}{\Gamma_{RD}} + \frac{\Gamma_{DR} \Gamma_{RL}}{\Gamma_{DL}} \right) + \mathcal{O} \left(\frac{\Gamma_{ij}^2}{\Gamma_D^2} \right). \quad (1.31)$$

We observe that in the lowest and next to lowest orders in the parameter Γ_{ij}/Γ_D the ratio w^* does not depend on \mathcal{F} and thus the FT holds. Comparing Eqs. (1.29) and (1.31) we note that within the accuracy of our approximation, i.e. up to the terms $\sim 1/\Gamma_D$, the ratio w^* may be written in the same form as for an ideal detector but with modified tunnel rates,

$$w^* \approx \frac{\Gamma_+(0)}{\Gamma_-(0)} = \frac{\Gamma_{DR}^* \Gamma_{RL}^* \Gamma_{LD}^*}{\Gamma_{LR}^* \Gamma_{RD}^* \Gamma_{DL}^*}, \quad (1.32)$$

and effective temperature

$$T^* = \frac{eV_S}{k_B \ln w^*}. \quad (1.33)$$

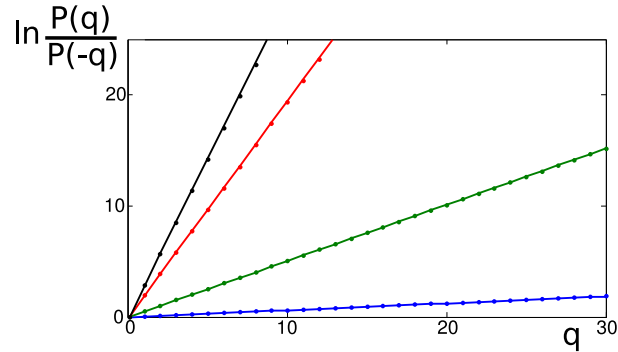


Fig. 1.6. The ratio of the probability of transferred charge as a function of the number of charges in the long-time limit. The solid lines are the results given by the analytical expression for the effective temperature [see Eq. (1.33)], the dots are from fully numerical calculations. The different colors correspond to different rates for the detector bandwidth: (black) $\Gamma_D = 100$ kHz, (red) $\Gamma_D = 10$ kHz, (green) $\Gamma_D = 1$ kHz, (blue) $\Gamma_D = 0.1$ kHz. The rates for the transitions on the dot are the same as used in Ref.¹⁸ and are of the order of 1 kHz: $\Gamma_{DR} = 4$ kHz, $\Gamma_{RD} = 0.3$ kHz, $\Gamma_{DL} = 1$ kHz, $\Gamma_{LD} = 1.5$ kHz, $\Gamma_{LR} = 1.7$ kHz, and $\Gamma_{RL} = 1.8$ kHz.

In the opposite limit of a slow detector, $\Gamma_D \ll \Gamma_{ij}$, one can show that $\mathcal{F} \sim \Gamma_D \ll \Gamma_{ij}$ and therefore one can put $\mathcal{F} = 0$ in Eq. (1.30). Surprisingly, this means that Eqs. (1.32-1.33) also become valid in the opposite limit, that of a very slow detector. Numerical calculations of \mathcal{F} confirm these results, but as expected \mathcal{F} does not have the right symmetries for intermediate values of Γ_D .

In Fig. 1.6 we compare our result for the effective temperature with numerical results. Varying the detector bandwidth over four orders of magnitude we see that our expression for the effective temperature Eq. (1.33) provides good fits for rather wide range of parameters of q and Γ_D . This means that although formally the detector model introduced by Naaman and Aumentado violates the FT, practically, the finite bandwidth effect can be accounted for simply by the effective temperature. Thus Eqs. (1.32-1.33) should describe the experiment reasonably well, regardless of the value of Γ_D .

To conclude, in this section we have demonstrated that a finite detector bandwidth in general distorts the measured statistics of the charge transfer and leads to the formal violation of FT. However the effect of the finite bandwidth can be accounted for by using the expression (1.33) for the effective temperature.

14 *Y. Utsumi*¹, *D. S. Golubev*², *M. Marthaler*³, *T. Fujisawa*^{4,5}, and *Gerd Schön*^{2,3}

1.6. Tunneling rates in the experiment

Let us now discuss how to determine the values of Γ_{ij} and Γ_D from experimental data. The standard way of doing this is to generate dwell time histograms for every current state. Let us consider the QPC current state corresponding to the DQD state $|L\rangle$. One should count how many times during sufficiently long observation time the QPC current has switched from the state $|L\rangle$ to either state $|R\rangle$ or $|D\rangle$ within the time interval from τ and $\tau + \Delta\tau$, where $\Delta\tau$ is sufficiently short. Denoting the corresponding numbers $\Delta N_{L \rightarrow R}$ and $\Delta N_{L \rightarrow D}$, one gets the histograms plotting the values $\Delta N_{L \rightarrow R, L \rightarrow R}(\tau)$ as a function of time τ . At sufficiently long time τ the numbers $\Delta N_{L \rightarrow R, L \rightarrow R}(\tau)$ decay in time exponentially,

$$\Delta N_{L \rightarrow R}(\tau) = K_{RL} e^{-\Gamma_L^* \tau}, \quad \Delta N_{L \rightarrow D}(\tau) = K_{DL} e^{-\Gamma_L^* \tau}. \quad (1.34)$$

The parameters Γ_L^* , K_{RL} and K_{DL} are extracted by fitting the histograms.

In the case of a fast detector, $\Gamma_D \gg \Gamma_{ij}$ one can easily express the DQD tunneling rates Γ_{RL} and Γ_{DL} in terms of the parameters Γ_L^* , K_{RL} , K_{DL} . Indeed, the theory in this case predicts $\Gamma_L^* = \Gamma_{RL} + \Gamma_{DL}$ and $K_{RL}/K_{DL} = \Gamma_{RL}/\Gamma_{DL}$ and, therefore

$$\Gamma_{RL} = \frac{K_{RL}}{K_{RL} + K_{DL}} \Gamma_L^*, \quad \Gamma_{DL} = \frac{K_{DL}}{K_{RL} + K_{DL}} \Gamma_L^*. \quad (1.35)$$

The remaining four rates are determined analogously.

In the following, we will present our analysis in detail. Suppose at time $\tau = 0$ the QPC current has switched to the state L . Since the state of the DQD remains unknown, the total occupation probability of such a state is given by the sum $p_L = p_{LL} + p_{RL} + p_{DL}$. To find out how this probability decays in time we have to solve the equation for the probabilities $\mathbf{p}^T = (p_{LL}, p_{RL}, p_{DL})$,

$$\partial_t \mathbf{p} = (\mathbf{\Gamma}(0) - \mathbf{\Gamma}_{D2} - \mathbf{\Gamma}_{D3}) \mathbf{p}. \quad (1.36)$$

This equation is a sub-block of a more general equation (1.23) where only the outgoing processes from the QPC state L are kept. For a large number of events the histograms should converge to the following expressions

$$\Delta N_{L \rightarrow R}(\tau) = N \Gamma_{DPRL}, \quad \Delta N_{L \rightarrow D}(\tau) = N \Gamma_{DPDL}, \quad (1.37)$$

where N is the normalization factor. Solving the differential equation and considering the long-time limit we arrive at Eqs. (1.34) with

$$\Gamma_L^* = \Gamma_{RL} + \Gamma_{DL} - \frac{\Gamma_{RL} \Gamma_{LR} + \Gamma_{DL} \Gamma_{LD}}{\Gamma_D} + \mathcal{O}\left(\frac{1}{\Gamma_D^2}\right) \quad (1.38)$$

and

$$\frac{K_{RL}}{K_{DL}} = \frac{\Gamma_{RL}^*}{\Gamma_{DL}^*} + \mathcal{O}\left(\frac{1}{\Gamma_D^2}\right). \quad (1.39)$$

Thus the ratio of the prefactor is sufficient to estimate the effective temperature (1.33).

One can also obtain the full time-dependence of $\Delta N_{L \rightarrow R}(\tau)$ and $\Delta N_{L \rightarrow D}(\tau)$. To this end we put $p_{LL}(0) = 1, p_{RL}(0) = p_{DL}(0) = 0$ and in the limit $\Gamma_D \gg \Gamma_{ij}$ obtain the result

$$\Delta N_{L \rightarrow R} = \frac{N\Gamma_D[\Gamma_{RL}(\Gamma_D + \Gamma_{LD} + \Gamma_{RD} - \Gamma_L^*) + \Gamma_{RD}\Gamma_{DL}][e^{-\Gamma_L^*\tau} - e^{-\Gamma_D\tau}]}{(\Gamma_D + \Gamma_{LR} + \Gamma_{D2} - \Gamma_L^*)(\Gamma_D + \Gamma_{LD} + \Gamma_{RD} - \Gamma_L^*) - \Gamma_{DR}\Gamma_{RD}},$$

$$\Delta N_{L \rightarrow D} = \frac{N\Gamma_D[\Gamma_{DL}(\Gamma_D + \Gamma_{LR} + \Gamma_{DR} - \Gamma_L^*) + \Gamma_{DR}\Gamma_{RL}][e^{-\Gamma_L^*\tau} - e^{-\Gamma_D\tau}]}{(\Gamma_D + \Gamma_{LR} + \Gamma_{D2} - \Gamma_L^*)(\Gamma_D + \Gamma_{LD} + \Gamma_{RD} - \Gamma_L^*) - \Gamma_{DR}\Gamma_{RD}}.$$

With the aid of these expressions one can extract Γ_D from the experimental data.

1.7. Summary

We have discussed the possibility of experimental verification of the FT (1.2) in single-electron counting experiments. Although the experiments allow testing the FT, the properties of the detector turn out to be very important. We have shown that in a generic system of a double quantum dot the FT (1.2) is robust against the backaction of a QPC detector in the sense that the effect of the latter can be absorbed in an effective temperature (1.11). We also investigated the influence of the finite bandwidth of the detector. We found that finite bandwidth results in the distortion of the signal properties and formally cannot be reduced to the renormalization of the effective temperature in Eq. (1.2). However, in practice these deviations turn out to be small, and Eq. (1.2) with modified temperature (1.33) should describe the data quite well, even if they are obtained with a slow detector. We hope the experimental test of the FT in the single-electron transport,¹⁸ as well as that in the Aharonov-Bohm ring,¹⁹ would stimulate the development in the nonequilibrium statistical physics and the mesoscopic quantum physics.

1.8. Acknowledgement

We thank M. Hettler, K. Kobayashi, and K. Saito for valuable discussions. This work has been supported by Strategic International Cooperative Pro-

16 Y. Utsumi¹, D. S. Golubev², M. Marthaler³, T. Fujisawa^{4,5}, and Gerd Schön^{2,3}

gram of the Japan Science and Technology Agency (JST) and by the German Science Foundation (DFG).

References

1. D. J. Evans, E. G. D. Cohen, and G. P. Morriss, Phys. Rev. Lett **71**, 2401 (1993).
2. J. L. Lebowitz and H. Spohn, J. Stat. Phys. **95**, 333 (1999).
3. D. Andrieux and P. Gaspard, J. Stat. Mech. P01011 (2006).
4. D. Andrieux and P. Gaspard, J. Stat. Phys. **127**, 107 (2007).
5. J. Kurchan, cond-mat/0007360.
6. J. Tobiska and Yu. V. Nazarov, Phys. Rev. B **72**, 235328 (2005).
7. M. Esposito, U. Harbola, and S. Mukamel, Phys. Rev. B **75**, 155316 (2007).
8. H. Förster and M. Büttiker, Phys. Rev. Lett. **101**, 136805 (2008).
9. K. Saito and Y. Utsumi, Phys. Rev. B **78**, 115429 (2008).
10. Y. Utsumi and K. Saito, Phys. Rev. B **79**, 235311 (2009).
11. D. Andrieux, P. Gaspard, T. Monnai, and S. Tasaki, New J. Phys. **11**, 043014 (2009).
12. C. Jarzynski, Phys. Rev. Lett. **78**, 2690 (1997).
13. M. Campisi, P. Talkner, and P. Hänggi, Phys. Rev. Lett. **102**, 210401 (2009).
14. G. Gallavotti, Phys. Rev. Lett. **77**, 4334 (1996).
15. G. M. Wang, E. M. Sevick, E. Mittag, D. J. Searles, and D. J. Evans, Phys. Rev. Lett. **89**, 050601 (2002).
16. J. Liphardt, S. Dumont, S. B. Smith, I. Tinoco Jr., C. Bustamante, Nature **296**, 1832 (2002).
17. Y. Imry, *Introduction to Mesoscopic Physics* (Oxford University Press, Oxford, 1997) 2nd ed.
18. Y. Utsumi, D. S. Golubev, M. Marthaler, K. Saito, T. Fujisawa, and G. Schön, arXiv:0908.0229.
19. S. Nakamura, Y. Yamauchi, M. Hashisaka, K. Chida, K. Kobayashi, T. Ono, R. Leturcq, K. Ensslin, K. Saito, Y. Utsumi, A. C. Gossard, arXiv:0911.3470.
20. T. Fujisawa, T. Hayashi, R. Tomita, and Y. Hirayama, Science **312**, 1634 (2006).
21. O. Naaman and J. Aumentado, Phys. Rev. Lett. **96**, 100201 (2006).
22. S. Gustavsson, R. Leturcq, T. Ihn, K. Ensslin, R. Reinwald, and W. Wegscheider, Phys. Rev. B **75**, 075314 (2007).
23. C. Flindt, C. Fricke, F. Hohls, T. Novotny, K. Netocny, T. Brandes, and R.J. Haug, Proc. Natl. Acad. Sci. USA **106**, 10116 (2009)
24. S. Gustavsson, R. Leturcq, M. Studer, I. Shorubalko, T. Ihn, K. Ensslin, D.C. Driscoll, A.C. Gossard, Surface Science Reports **64**, 191 (2009).
25. D. A. Bagrets and Yu. V. Nazarov, Phys. Rev. B **67**, 085316 (2003); D.A. Bagrets, Y. Utsumi, D.S. Golubev, and G. Schön, Fortschritte der Physik **54**, 917 (2006).
26. J. Schnakenberg, Rev. Mod. Phys. **48**, 571 (1976).

27. U. Gasser, S. Gustavsson, B. Küng, K. Ensslin, T. Ihn, D. C. Driscoll, and A. C. Gossard, *Phys. Rev. B* **79**, 035303 (2009).
28. M. Hashisaka, Y. Yamauchi, S. Nakamura, S. Kasai, T. Ono, and K. Kobayashi, *Phys. Rev. B* **78**, 241303(R) (2008).
29. R. Aguado and L. P. Kouwenhoven, *Phys. Rev. Lett.* **84**, 1986 (2000).
30. G.-L. Ingold and Y. V. Nazarov, in *Single Charge Tunneling*, eds. H. Grabert and M. Devoret, NATO ASI, Series B: Physics (Plenum, N.Y., 1992), Vol. 294, pp. 21-107.
31. J. König, H. Schoeller, and G. Schön, *Phys. Rev. Lett.* **76**, 1715 (1996); J. König, J. Schmid, H. Schoeller, and G. Schön, *Phys. Rev. B* **54**, 16820 (1996).
32. D. V. Averin and E. V. Sukhorukov, *Phys. Rev. Lett.* **95**, 126803 (2005).